Modulation of Angiogenesis by Genetic Manipulation of ATF4 in a Mouse Modulation of Angiogenesis by Genetic Manipulation

Xiaoqin Wang,[1] Guibo Wang,[1] Mansi Kunte,[1] Vishal Shinde,[2] and Marina Gorbatyuk[2]

[1]Department of Cell Biology and Anatomy, University of North Texas Health Science Center, North Texas Eye Research Institute, Fort Worth, Texas
[2]Department of Vision Sciences, University of Alabama at Birmingham, Birmingham, Alabama

Correspondence: Marina Gorbatyuk, Department of Vision Sciences, University of Alabama at Birmingham, 1670 University Boulevard, Birmingham, AL 35294; mgortk@uab.edu.

XW and GW contributed equally to the work presented here and should therefore be regarded as equivalent authors.

Submitted: March 28, 2013
Accepted: August 5, 2013

Citation: Wang X, Wang G, Kunte M, Shinde V, Gorbatyuk M. Modulation of angiogenesis by genetic manipulation of ATF4 in a mouse model of oxygen-induced retinopathy. *Invest Ophthalmol Vis Sci*. 2013;54:5995–6002. DOI:10.1167/iovs.13-12117

Purpose. The activation of the unfolded protein response (UPR) and an increase in activating transcription factor 4 (ATF4) has been previously reported in the diabetic retina. Despite this, a direct link between ATF4 and the degree of proliferative retinopathy has not been demonstrated to date. Therefore, the objective of this study was to determine whether ATF4 deficiency could reduce neovascularization in mice with oxygen-induced retinopathy (OIR).

Methods. We induced OIR in C57BL/6, ATF4$^{+/-}$, and endoplasmic reticulum stress–activated indicator (ERAI) mice and used quantitative RT-PCR and Western blot analysis to evaluate relative gene and protein expression. Histology and microscopy were used to calculate the extent of neovascularization in flat-mounted retinas.

Results. Experimental data revealed Xbp1 splicing in the retinal ganglia cells, outer plexiform layer, inner nuclear layer, and outer nuclear layer and in pericytes of postdevelopment day 17 ERAI OIR mice, confirming the activation of IRE1 UPR signaling. In naive ATF4-deficient mice, we also observed an elevation in UPR-associated and vascular-associated gene expression (*Bip*, *Atf6*, *Hif1a*, *Pik3/Akt*, *Flt1/Vegfa*, and *Tgfb1*), which may have contributed to the alleviation of hypoxia-driven neovascularization in experimental ATF4$^{+/-}$ retinas. The OIR ATF4$^{+/-}$ retinas demonstrated reprogramming of the UPR seen at both the mRNA (*Atf6* and *Bip*) and protein (pATF6 and peIf2α) levels, as well as a reduction in vascularization-associated gene expression (*Flt1*, *Vegf1*, *Hif1*, and *Tgb1*). These changes corresponded to the decline in the rate of neovascularization.

Conclusions. Our study validates ATF4 as a prospective therapeutic target to inhibit neovascularization in proliferative retinopathy.

Keywords: oxygen-induced retinopathy, angiogenesis, unfolded protein response, activating transcription factor 4, vascular endothelial growth factor

Diabetic retinopathy (DR) is a major complication in patients with diabetes that affects about 8.3% of the US population (http://www.diabetes.niddk.nih.gov/dm/pubs/statistics/#fast [in the public domain]) and can lead to severe visual impairment.[1,2] Although the precise mechanisms of DR onset and progression are still under investigation, recent studies[3,4] have indicated that the activation of the unfolded protein response (UPR) could be one of the major players.

Initiation of the UPR occurs through the activation of the following three UPR signaling arms: RNA-dependent protein kinase (PKR)-like endoplasmic reticulum (ER) kinase (PERK), inositol-requiring protein 1 (IRE1), and activating transcription factor 6 (ATF6). The molecular chaperone immunoglobulin heavy chain–binding protein (GRP78/BIP) represses all three mediators when the cell is in normal homeostasis by tightly binding to them. When ER homeostasis is disturbed during hypoxia[5,6] and unfolded proteins accumulate in the ER lumen, BiP dissociates from the above-mentioned mediators, thus initiating the UPR. These mediators exert their influence primarily via the transcription factors activating transcription factor 4 (ATF4), X-box–binding protein 1 (XBP1), and ATF6, which represent the PERK, ATF6, and IRE UPR arms, respectively. During the activation of IRE1 signaling, a 26-base pair (bp) fragment is excised from the XBP1 message, thus producing the active spliced variant of Xbp1, which in turn activates multiple genes crucial for secretion and protein folding. The activation of the ATF6 arm occurs through the phosphorylation and cleavage of its namesake protein, resulting in a 50-kilodalton pATF6 protein. Similarly, PERK activation also results in the phosphorylation of eukaryotic initiation factor 2 subunit α (eIF2α), which inhibits global mRNA translation, while inducing transcription of ATF4. This latter mediator translocates to the nucleus, where it activates a third set of UPR target genes, resulting in transcriptional upregulation of the proapoptotic CHOP protein.

The UPR hallmark ATF4 can function both as a transcriptional activator and repressor. It has been previously described as having a role in cellular adaptation to stress such as ER or oxidative stress,[7] as well as being a necessary component of skeletal, eye, and hematopoietic development.[8] Roybal et al.[8] have demonstrated that the ATF4 complex is able to bind to the intronic amino acid response element site within the VEGF

gene and transactivate gene expression. In retinal Müller cells, it has been demonstrated that ATF4 overexpression is sufficient to induce VEGF expression; conversely, inhibition of ATF4 significantly attenuates hypoxia-associated VEGF induction, which is known to be a hallmark of proliferative DR.[9] All of these findings indicate that the ATF4 gene is a novel therapeutic target for the regulation of angiogenesis via its influence on VEGF expression.

Various rodent models have been used to study the molecular mechanisms underlying the pathogenesis of DR.[10] However, one major criticism of these models is that they may not exactly mirror the phenotype of human DR, especially with regard to the extent of DR pathology. Diabetic retinopathy chemically induced by streptozotocin (STZ) is a widely used model to develop type 1 diabetes mellitus. In STZ- induced diabetic mice, the role of ATF4 was tested by genetic modulation of ATF4 in a recent study.[11]

Compared with STZ-induced DR, the oxygen-induced retinopathy (OIR) mice together with Kimba and transgenic mice overexpressing IGF1 exhibit neovascularization, which is also seen in the end stage of DR.[10,12,13] The following two phases are involved in pathological neovascularization in the OIR retina: hyperoxia, which is induced by supplementation with oxygen and is characterized by the suppression of VEGF, and hypoxia, which is created by returning pups with avascular retina to room air at postdevelopment day (P) 12. The latter condition triggers an increase in Hif1a, VEGF production, and both normal vessel growth and a pathological neovascular response.[14] At this point in the study of diabetic DR, despite the demonstration of a relationship between an increase in neovascularization and ER stress, the role of ATF4 in the promotion of neovascularization has not been explored.

Elevated expression of Grp78 and ATF4 and the phosphorylation of eIf2α have been detected in the OIR retina,[13] suggesting that ER stress is enhanced during OIR. Moreover, the precise role of UPR activation has been studied in experimental OIR with mild ER stress. It has been shown that the activation of ER stress promotes retinal neovascularization in OIR mice via induction of Bip/Grp78, a key UPR protein.[15] Exposure to tunicamycin and thapsigargin, both ER stress inducers, in these retinas accelerates retinal neovascularization, thus confirming the contribution of ER stress in the formation of abnormal vasculature.[15]

Taking into account that the reduction of one copy of ATF4 markedly attenuates the high glucose–induced production of VEGF and reduces vascular leakage in the retinal homogenate of STZ diabetic mice and given the lack of studies elucidating the effect of ATF4 on the degree of neovascularization in late-stage DR, we wanted to determine if there was a direct link between the levels of ATF4 and the size of the area affected by neovascularization in OIR mice. We demonstrated that manipulation of ATF4 and the resulting suppression of UPR markers could be beneficial for the prevention of angiogenesis in the retina. We also established that this approach could be undertaken as a therapeutic strategy for the treatment of DR and ischemic vascular diseases through a reduction in the extent of neovascularization.

Materials and Methods

Animals

C57BL/6, ATF4-deficient ($ATF4^{+/-}$), and ER stress–activated indicator (ERAI) mice were used for this study. The animal protocol was approved by the University of North Texas Health Science Center Animal Care and Use Committee and was conducted following animal guidelines according to the ARVO Statement for the Use of Animals in Ophthalmic and Vision Research. All animals were reared with 12-hour day and night cycles. To demonstrate that hypoxia induces the activation of the UPR, we used ERAI transgenic mice (Riken Bioresource Center, Kumagaya City, Japan), which carry a human XBP1 and venus (a variant of green fluorescent protein) fusion gene under control of a CAG promoter. The transcripts from ERAI constructs are spliced under ER stress. The spliced mRNA is translated into an XBP1-venus fusion protein. These mice were used in our previous study[16] demonstrating the activation of IRE1 signaling in the retina through the splicing of the Xbp1 mRNA and the expression of a resulting XBP1-GFP fusion protein. In this study, we used the same mice to create a model for OIR and demonstrated a distribution of GFP across the retina. To subsequently demonstrate that ATF4 knockdown can rescue the hypoxia-induced phenotype, the $ATF4^{+/-}$ and C57BL/6 mice were exposed to hyperoxia by subjecting mouse pups with their nursing mothers to 75% oxygen in an oxygen chamber (Coy Lab Products, Grass Lake, MI) between P7 and P12 as previously described.[14,17] On P12, mouse pups were returned to room air, and the avascular retina became hypoxic, triggering both normal vessel regrowth and a pathological neovascular response.[14] This hypoxic phase induces a rapid increase in hypoxia-inducible factor (HIF)–regulated growth factor VEGF.[14] Naive $ATF4^{+/-}$ and C57BL/6 mice were used as controls to corresponding OIR groups. At P13, P15, or P17, pups were anesthetized by carbon dioxide and killed by cervical dislocation, and the retinas were enucleated. Mouse tails were collected, and DNA was extracted using a 2.0× Taq RED Master Mix Kit (Apex, San Diego, CA).

Genotyping

To identify the ERAI genotype, PCR was performed as previously described.[16] To identify $ATF4^{+/-}$, the following three primers were used: common primer one (GTT TCT ACA GCT TCC TCC ACT CT), C57BL/6 primer two (CAT ACT GGC TTT GTG CCA GA), and mutant primer three (ATT AAG GGC CAG CTC ATT CC). Primer one and primer two amplify 465-bp fragments, and primer one and primer three amplify 354-bp fragments. The presence of two bands indicated a positive result.

Histology and Immunohistochemistry

After the eyes were enucleated, the cornea, iris, and sclera were removed, leaving the retina around the lens. The eyes were fixed in 4% paraformaldehyde (PFA) for 1 hour at 4°, and the lens was removed. The whole retinas were then fixed in 4% PFA for an additional 2 hours at 4°. Fixed samples were rinsed with PBS at room temperature. The eyes were cut to the edge of the cornea with scissors, the sclera was pulled off, and the retina was cut into four parts like a flower and transferred to new well to start staining. Retinal flat mounts were stained in 100 μL of 1 mg/mL of lectin (DL-1177; Vector Labs, Inc., Burlingame, CA) overnight. To avoid amplifying autofluorescence and to demonstrate specificity for GFP detection, we used an anti-GFP antibody (Abcam, Cambridge, MA). On the next day, flat mounts were dyed with 4′,6-diamidino-2-phenylindole (DAPI) and observed under a fluorescence microscope (Zeiss, Oberkochen, Germany). The retinas were photographed with the fluorescent microscope and merged to obtain whole-mount retinal images using Photoshop CS3 (Adobe Systems, Inc., San Jose, CA). For cryosections, the eyes were fixed the same way, embedded in optimum temperature cutting compound, cut into 7-μm slices, and stained using the above procedure in conjunction with propidium iodide.

Quantification of Neovascularization

Retinal images were analyzed using Photoshop CS3. The total surface area and the area without vasculature (empty space) were measured. Neovascularization was calculated at P17 as the difference between the total area and the empty space. Ten sections from each group were examined. The average amount of neovascular area was compared with that of the control group using the Student's *t*-test.

Real-Time PCR and Western Blot

The RNA and protein extracts from P12, P13, and P15 retinas were prepared as previously described.[18] We used a custom Taqman array plate with 16 genes, including *Gapdh* endogenous controls (Applied Biosystems, Carlsbad, CA). The RT-PCR was performed using approximately 50 ng of cDNA mixed with TaqMan universal PCR master mix and the StepOnePlus Real-time PCR system (both from Applied Biosystems). The following four groups of animals were used: ATF4$^{+/-}$ and C57BL/6 naive mice and ATF4$^{+/-}$ and C57BL/6 OIR mice. The results were analyzed by two-way ANOVA using GraphPad Prism (GraphPad Software, Inc., La Jolla, CA).

Total protein was extracted from all four groups at P13, and 40 to 70 μg of total protein was loaded on 12% SDS-PAGE gels (Biorad, Hercules, CA). Specific antibodies were used to detect VEGFa (Santa-Cruz Biotechnology, Inc., Santa Cruz, CA), BiP (Santa-Cruz Biotechnology), CHOP (Abcam), ATF6 (Imgenex Corp., San Diego, CA), and pEif2α (Cell Signaling Technology, Danvers, MA). The membrane was then stripped, and β-actin was detected as an internal control. Protein detection was performed using an infrared secondary antibody and an Odyssey infrared imager (LI-COR Biosciences, Inc., Lincoln, NE).

Results

Area of Neovascularization Is Reduced in the ATF4$^{+/-}$ OIR Mice

To demonstrate the activation of the UPR in the OIR flat-mounted retina, we performed experiments with P17 ERAI retina that carried the Xbp1-GFP transgene (Fig. 1) and identified the splicing of Xbp1-GFP visualized by fluorescent microscopy. For example, ERAI cryosections exhibited GFP all over the retina, including in retinal ganglia cells (RGCs), the outer plexiform layer, and the outer and inner nuclear layers. This finding indicates that by P17 in ORI retinas the ER stress activation occurred not only in the RGCs but also in other retinal cell types, including photoreceptors. Figure 1 also shows that pericytes expressed GFP in the ERAI OIR retina, suggesting that the activation of the IRE1 signaling pathway occurred in these cells and not in pericytes of control retinas. All together, these data demonstrate the involvement of the IRE1 pathway in the mechanism of OIR.

We then analyzed retinal flat mounts of C57BL/6 OIR and ATF4$^{+/-}$ OIR mice and found that the ATF4$^{+/-}$ retinas had smaller areas of new neovascularization and larger avascular areas versus controls. The data were expressed as a ratio of neovascularization or avascular area to total examined area of individual retinas and are shown in Figure 2 and Supplementary Figures S1 and S2. For example, we found that the neovascularized area was less in ATF4$^{+/-}$ retinas (0.84 ± 0.01 in ATF4$^{+/-}$ and 1.00 ± 0.01 in C57BL/6). Conversely, the avascular area demonstrated a greater than 2.0-fold increase in ATF4-deficient retinas compared with control retinas (2.15 ± 0.09 in ATF4$^{+/-}$ and 1.00 ± 0.06 in C57BL/6).

Alteration of UPR-Induced and Vascularization-Induced Gene Expression During Retinal Development in ATF4$^{+/-}$ Retinas

Hypoxia in OIR mice decreases with ongoing retinal development and cell differentiation.[19] Endoplasmic reticulum stress has also been found to be a part of normal retinal and lens embryonic development.[20,21] In support of these findings, the results obtained in our laboratory suggest that the activation of the UPR occurs in rodent retinas during the first 2 weeks of life (data not shown). Therefore, given that the mouse retina experiences modulation of many genes during development[22] and that programmed cell death naturally occurs in the developing vertebrate retina,[23] we decided to dissect the role of hypoxia-driven alteration of gene expression in ATF4-deficient retinas from the effect of genetic manipulation with ATF4 in developing retinas and to analyze the UPR-associated gene expression in the ATF4$^{+/-}$ mice. The list of studied genes includes the UPR-associated *ATF6*, *CHOP* (DDIT3 or DNA damage–inducible factor 3), *Bip* (*Grp78*), *eIF2α*, *Xbp1*, *Bax* (BCL2-associated X protein), and *Hif1α*, all of which were shown to be modulated in DR.[4,13,24] A major role of phosphatidylinositide kinases/v-akt murine thymoma viral oncogene (protein kinase B) (Pi3K/AKT) signaling has been described in the induction of angiogenesis and the prolonging of cellular survival in the proliferative stage of DR[25] and therefore was also tested in this study. Our selection of the mitogen-activated protein kinase 3 (or ERK1) (MAPK3) was based on ERK1 involvement in VEGF release in diabetic retinas.[26,27] For this reason, we studied the *Mapk3* gene, along with *Vegfα*, *Flt1* (VEGF receptor 1), and *Pik3r1* (phosphoinositide-3-kinase, regulatory subunit 1). *Tgfβ1* (transforming growth factor β1) expression and secretion have been shown to increase in diabetic retinas and were thus also of interest to us. *Tgfβ1* was also proposed together with VEGF and IGF1 to stimulate residual vessel proliferation.[28] In addition, we selected this factor based on the proposed link between ATF4 ablation and downregulation of TGFb expression in neuronal cells.[29]

Analysis of gene expression (Fig. 3, Supplementary Table S1) showed that P12 ATF4-deficent retinas had a 2.3-fold increase in *Akt* expression, a 3.0-fold increase in *Atf6* expression, a 2.4-fold increase in *Bax*, a 2.7-fold increase in *Bip*, and a 3.6-fold increase in *Mapk3*. The *eIf2a*, *Xbp1*, and *Chop* gene expression did not significantly differ in ATF$^{+/-}$ mice versus controls at P12. The P12 ATF4-deficient retinas also demonstrated a 4.7-fold upregulation of the *Hif1a* gene compared with controls. Vascularization-related gene expression was also modified and exhibited increases of 3.3-fold in *Flt1* and 4.0-fold in *Pik3r1*, as well as 2.0-fold and 3.8-fold increases in the *Tgb1* and *Vegfa* genes, respectively.

At P13, ATF4-deficent retina showed a 3.2-fold increase in *Atf6* expression and a 3.6-fold increase in *Hif1a* gene expression. Gene expression of *eIf2a*, *Xbp1*, *Chop*, *Bip*, Akt, *Bax*, *Mapk3*, and *Nfkb* did not significantly differ in ATF4$^{+/-}$ mice compared with controls. The expression of vascularization-related genes such as *Flt1* and *Pik3r1* was upregulated by 3.6-fold and 3.1-fold, respectively, in ATF4$^{+/-}$ retinas. The expression of *Tgfb1* and *Vegfa* was not different from that in controls at P13.

At P15, we determined that the expression of UPR-associated genes was not statistically different in ATF4$^{+/-}$ mice versus controls. Only *Mapk3* expression was significantly upregulated by 1.5-fold in P15 ATF4$^{+/-}$ retinas. Vascularization-related genes such as *Flt1* and *Tgfb1* were upregulated by 1.9-fold and 2.0-fold, respectively, while the expression of *Vegfa* and *Pik3r1* did not differ from that in controls.

Investigative Ophthalmology & Visual Science

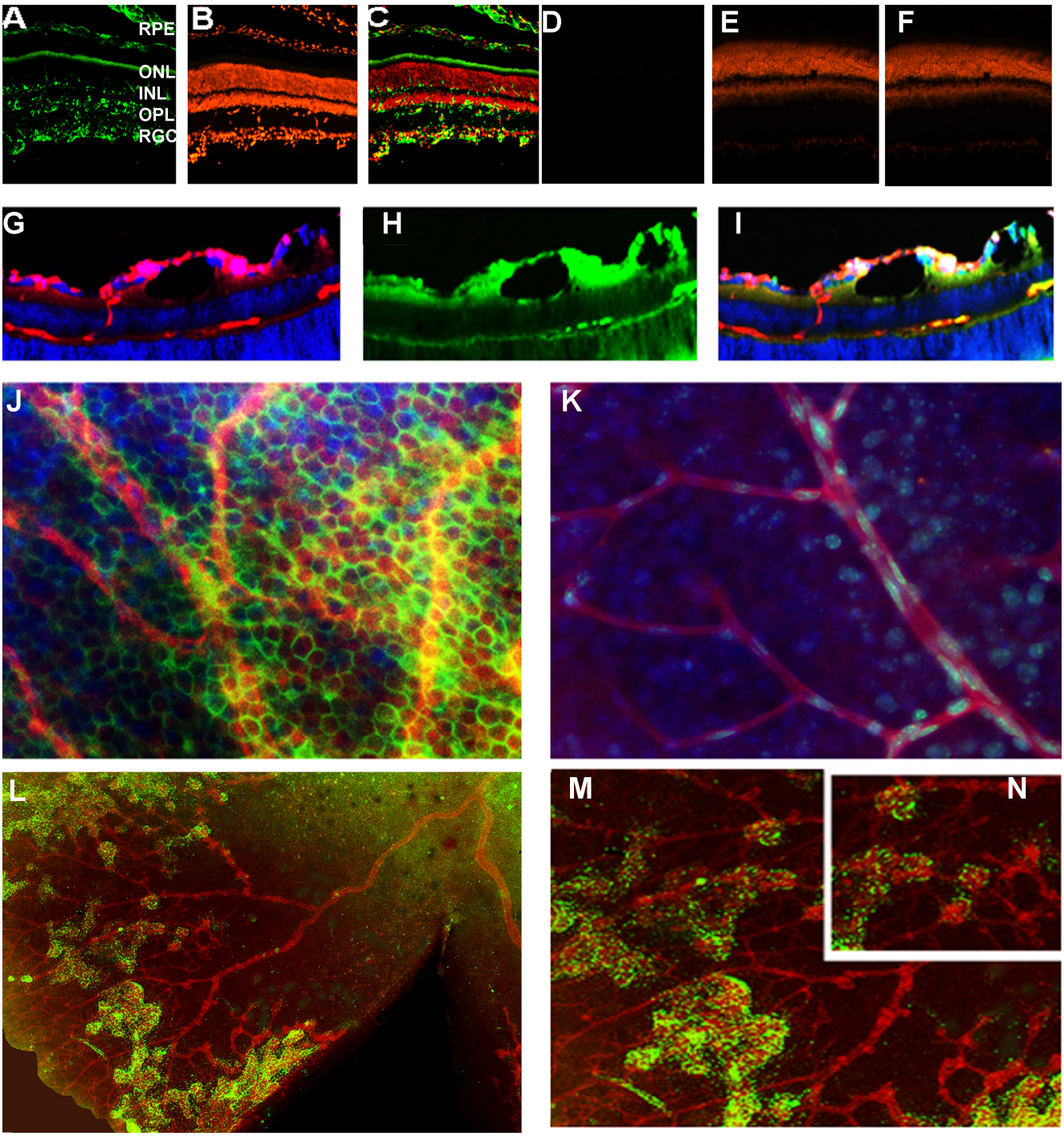

Figure 1. Unfolded protein response is activated in the ERAI OIR retina. (**A–F**) The expression of the spliced Xbp1-GFP was detected in retinal cryosections in the RGCs, outer plexiform layer, outer nuclear layer, and inner nuclear layer in P17 ERAI OIR compared with naive ERAI. Nuclei were stained with propidium iodide (*red*), and the GFP protein (*green*) was detected by immunohistochemistry with antibody against GFP to avoid autofluorescence and increase our specificity of detection. (**E**, **G**, **H**, **I**) Formation of retinal blood vessels in the ERAI OIR mice. The retinal cryosections were stained overnight with lectin, a blood vessel marker (*red*). Detection of the GFP protein was observed in pericytes (*green*). Nuclei were stained with DAPI (*blue*). (**J**, **K**) The pericytes of the ERAI OIR blood vessel (**J**) experience the activation of the IRE signaling and the splicing of Xbp1 compared with pericytes in control ERAI retina (**K**). (**L**) Immunostaining of the ERAI IOR flat-mounted retina was performed using anti-lectin and anti-GFP antibodies; nuclei were stained with DAPI. (**M**) and (**N**) are high-resolution images of (**L**).

Investigative Ophthalmology & Visual Science

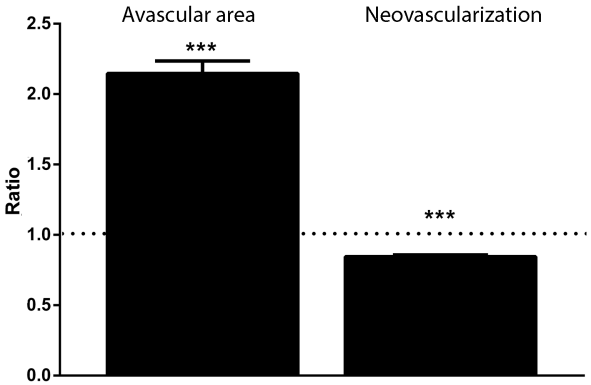

FIGURE 2. Area of neovascularization is reduced in ATF4$^{+/-}$ OIR mice. Neovascularized and avascular areas in C57BL/6 OIR ($n = 5$) and ATF4$^{+/-}$ OIR ($n = 5$) retinas were calculated for P17 retinal flat mounts. The ratio of neovascularization or avascular area to total examined area for individual retinas was used. A 15% reduction in new blood vessel formation and a 2.0-fold increase in the avascular area were detected in genetically modified retinas (***$P < 0.001$). The ratio of experimental group to control group is presented. Control groups are indicated with a *dashed line*. The images of control and experimental retinas are presented in Supplementary Figures S1 and S2.

Hypoxia-Driven Modulation of UPR-Associated and Vascular-Associated Gene Expression in ATF$^{+/-}$ Retinas

To avoid the potential effects of changing gene expression during development on the results of hypoxia-induced gene expression, we further express the results of RNA and protein analysis of C57BL/6 OIR and ATF4$^{+/-}$ OIR retinas as a ratio of relative quantification $(RQ)_{hypoxia}$ to $RQ_{normoxia}$. The results of quantitative RT-PCR analysis (Fig. 3, Supplementary Table S2) demonstrated that the expression of UPR-induced genes such as *Atf6*, *Bip*, and *Hif1a* was modified in ATF4$^{+/-}$ OIR retinas. For example, the levels of *Atf6* were significantly reduced by 50% at P12 but showed no difference compared with C57BL/6 retinas at P13 and P15, when C57BL/6 OIR mice also demonstrated a reduction in *Atf6*. At P12, we observed a 50% reduction in *Bip* gene expression in ATF4$^{+/-}$ OIR retinas, while at P13 and P15 there was no detectable difference. At P12, *Hif1a* expression was significantly reduced in ATF4$^{+/-}$ OIR retinas by almost 60%.

We found that the level of *Flt1* was significantly reduced by 55% in P12 ATF4$^{+/-}$ OIR retinas and correlated with a greater than 60% reduction in *Vegfa* expression at the same time point (Fig. 4). There was no significant difference between groups in *Flt1* and *Vegfa* expression at either P13 or P15. At P15, the expression of *Tgfb1* was reduced significantly by 60% in ATF4-deficient retinas, but no differences were detected earlier at P12 or P13.

The PERK and ATF6 Pathways Are Modulated in ATF4$^{+/-}$ OIR Retinas

We analyzed retinal protein extracts 24 hours after transferring mice to room air (P13). The results from this experiment are shown in Figure 5. The levels of BiP and Chop proteins in ATF4$^{+/-}$ OIR retinas did not differ from controls; however, the level of phosphorylated (p) IF2α, the hallmark of the PERK pathway, was significantly lower in ATF4$^{+/-}$ OIR retinas and was 0.94 ± 0.01 arbitrary units (a.u.) vs. 1.43 ± 0.11 a.u. in C57BL/6 OIR ($P = 0.01$). The level of pATF6 (50 kD) protein,

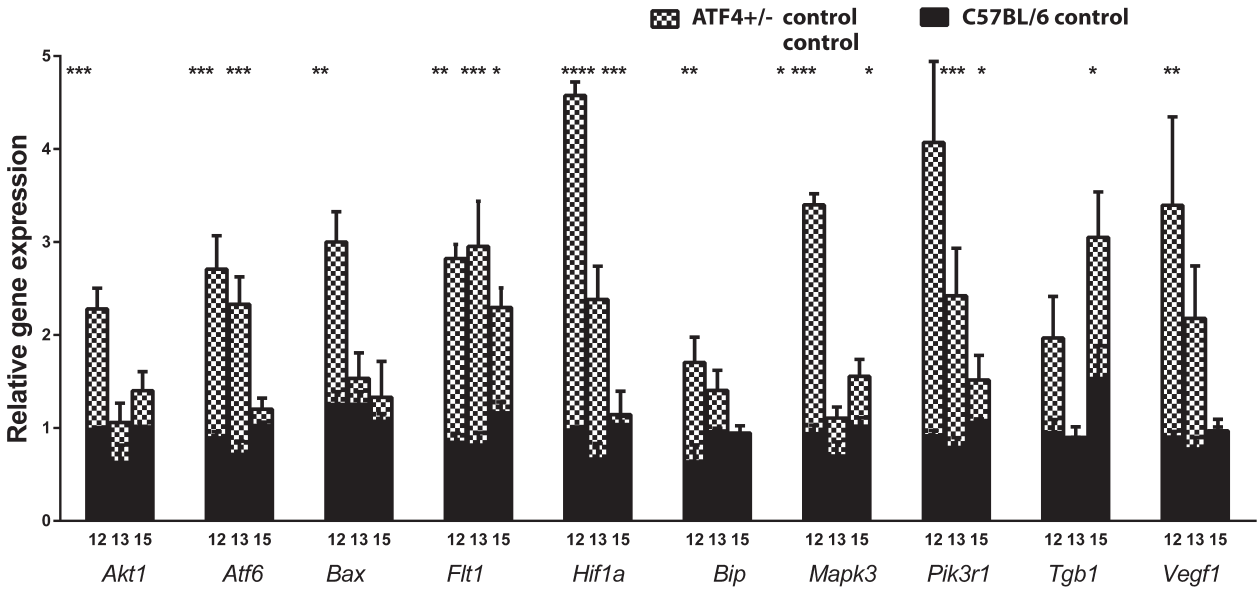

FIGURE 3. Alteration of UPR-induced and vascularization-related gene expression during retinal development in ATF4$^{+/-}$ mice. The relative gene expression was articulated in RQs and was calculated in C57BL/6 ($n = 4$) and ATF4$^{+/-}$ ($n = 4$) naive animals at P12, P13, and P15 using C57BL/6 controls as a reference at each time point. Two-way ANOVA was used to calculate the difference between groups. At P12, we observed a 2.3-fold increase in *Akt*, a 3.0-fold increase in *Atf6*, a 2.4-fold increase in *Bax*, a 2.7-fold increase in *Bip*, a 3.6-fold increase in *Mapk3*, and a 4.6-fold increase in *Hif1a* gene expression. At P13, the expression of these genes was back to control levels with the exception of *Hif1a* and *Atf6*; their expression was still elevated by 3.2-fold and 3.6-fold, respectively. At P15, the expression of UPR-induced genes did not differ from that of controls. Vascularization-related gene expression was also altered in ATF4$^{+/-}$ retinas during retinal development. For example, *Pik3r1* expression was increased by 4.4-fold and 3.1-fold at P12 and P13, respectively. By P15, its expression was back to control levels. While *Vegfa* and *Tgfb1* expression was upregulated only at P12 and P15 by 3.7-fold and 2.0-fold, respectively, the expression of *Flt1* was consistently elevated during the analyzed period and was 3.3-fold, 3.6-fold, and almost 2.0-fold higher in ATF4$^{+/-}$ mice at P12, P13, and P15, respectively. See also Supplementary Table S1 (*$P < 0.05$, **$P < 0.01$, ***$P < 0.001$, ****$P < 0.0001$).

Investigative Ophthalmology & Visual Science

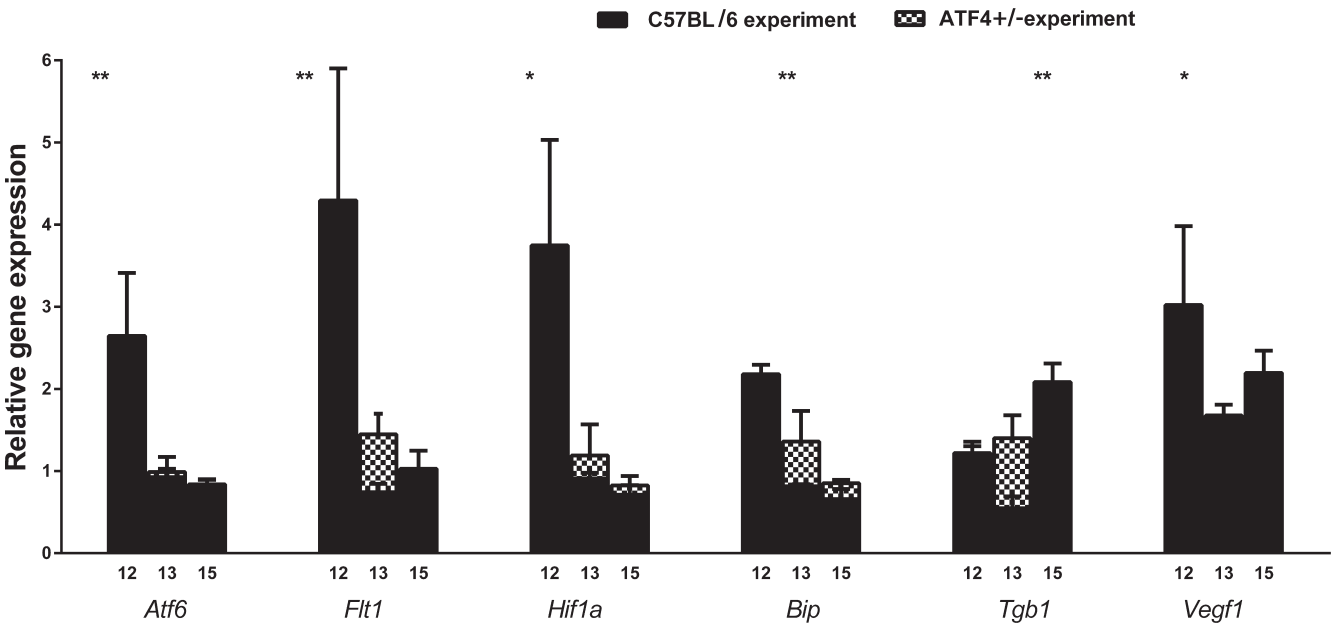

Figure 4. Hypoxia induces modulation of the expression in UPR-associated and vascularization-related genes in ATF4$^{+/-}$ retinas**.** The relative gene expression was articulated in RQs and was analyzed in C57BL/6 OIR ($n = 4$) and ATF4$^{+/-}$ OIR ($n = 4$) retinas at P12, P13, and P15 using a ratio of RQs in experimental groups to RQs in controls. Two-way ANOVA was used to calculate the difference between groups. Compared with C57BL/6 OIR, the ATF4$^{+/-}$ OIR mice experienced induction of the UPR at a much lower level. The level of *Atf6* and *Bip* gene expression was significantly reduced by 50% at P12. *Hif1* expression was diminished by almost 60% in ATF4$^{+/-}$ OIR retinas, despite the fact that in naive ATF4$^{+/-}$ animals *Hif1a* expression was elevated at P12. The level of *Flt1* was also significantly reduced by 55% in P12 ATF4$^{+/-}$ OIR retinas, which was in agreement with a greater than 60% reduction of *Vegfa* gene expression at the same time point. This could perhaps be responsible for the significant downregulation of *Tgfb1* (60%) in ATF4-deficient retinas at P15 (*$P < 0.05$, **$P < 0.01$, ***$P < 0.001$, **** $P < 0.0001$).

the hallmark of ATF6 signaling, was significantly reduced in ATF4$^{+/-}$ OIR retinas and was 1.00 ± 0.04 a.u. vs. 1.30 ± 0.04 a.u. ($P = 0.007$). The full-length pATF6 (90 kD) protein was also diminished (0.92 ± 0.02 a.u. in ATF4$^{+/-}$ vs. 1.25 ± 0.04 a.u. in C57BL/6, $P = 0.002$), suggesting that ATF6 and PERK signaling was reduced in ATF4$^{+/-}$ OIR mice. We also confirmed that VEGFa protein levels were reduced in ATF4$^{+/-}$ OIR retinas compared with controls (1.25 ± 0.04 a.u. in C57BL/6 vs. 1.00 ± 0.04 a.u. in ATF4$^{+/-}$, $P = 0.005$).

Discussion

The activation of the UPR has been previously shown in OIR mice. In the present study, we demonstrate that IRE signaling of the UPR is activated in the ERAI OIR retina through the promotion of Xbp1 splicing. This was most clearly demonstrated by the splicing of Xbp1 and the expression of the Xbp1-GFP fusion protein throughout the retina. The trigger role of ATF4 in promoting vascular permeability has been studied in STZ-induced diabetic ATF4$^{+/-}$ mice.[30] Herein, we demonstrat-

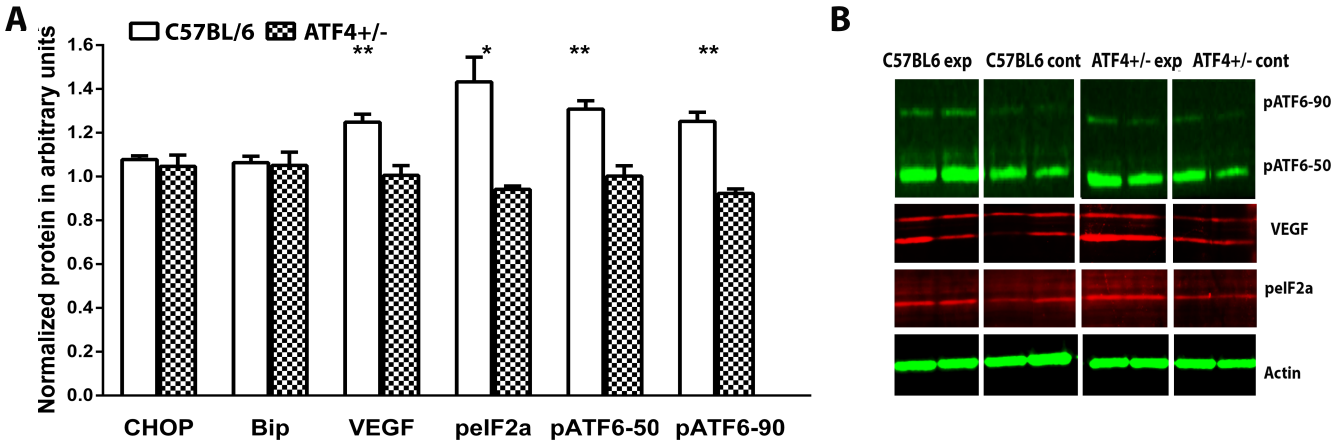

Figure 5. The PERK and ATF6 pathways are downregulated in ATF4$^{+/-}$ OIR retina**.** Retinal protein extracts were analyzed 24 hours after transferring mice to room air (P13). (**A**) Protein levels were analyzed in C57BL/6 OIR ($n = 4$) and ATF4$^{+/-}$ OIR ($n = 4$) retinas using a ratio of arbitrary units (a.u) in experimental groups to control groups. The Student's *t*-test was used to calculate differences in protein expression. While Bip and Chop protein expression was not modified in ATF4$^{+/-}$ OIR retinas, the levels of pIF2α (the hallmark of the PERK pathway), pATF6 (50 kD), and pATF6 (90 kD) (the ATF6 pathway) were significantly decreased in ATF4$^{+/-}$ OIR retinas by 20% ($P = 0.02$), 27% ($P = 0.001$), and 29% ($P = 0.002$), respectively. The VEGFa protein levels were reduced in ATF4$^{+/-}$ OIR retinas by 20% compared with controls ($P = 0.005$) (*$P < 0.05$, **$P < 0.01$). (**B**) Images of blots stained for pATF6, peIF2, VEGF, and β-actin.

ed that genetic manipulation with ATF4 could modulate the level of neovascularization and reprogram the UPR at both the mRNA and protein levels in proliferative retinopathy.

We analyzed the expression of genes that could potentially be linked to UPR induction or the promotion of neovascularization in the mouse retina and learned that ATF4-deficient retinas demonstrated upregulation of *ATF6* and *Bip* at P12 and P13. These time points are within the process of retinal development that begins during embryonic life and continue into the early postnatal days[31] and are characterized by apoptotic cell death[32] and the activation of the UPR.[20,21] For this reason, the induction of UPR genes at P12 is not a surprising observation. Apparently, the ATF4-deficient retinas experience either stronger activation of the UPR or delayed activation of the UPR compared with controls. In favor of the latter hypothesis, increased *Bip* and *Atf6* gene expression at P12 and P13 is restored back to normal by P15. In contrast, we also observed elevated *Hif1a* expression, which would support the hypothesis of ongoing UPR activation in P12 ATF4$^{+/-}$ control retinas. HIF1a and AKT share the ability to induce angiogenesis and consequently could be responsible for the increase in *Vegfa* and *Flt1* (*Vegfr1*) expression at this time point.[33–35] It is also possible that under conditions of ATF4 deficit *Vegfa* expression is compensated by the overexpression of *Hif1a*, leading to upregulation of *Flt1*. At P12, enhanced *Vegfa* could also be responsible for increased *MAPK3* expression.[36]

The VEGF-induced activation of the PI3K/Akt1 pathway has been previously reported.[36,37] It is therefore not surprising to observe the upregulation of *Pi3kr1*, which together with increased *Akt* points to the potential transient activation of the protective PI3K/AKT signaling[38] in developing ATF4$^{+/-}$ retinas, which could in turn lead to resistances against hypoxia-driven neovascularization. Recently, it was demonstrated that *Pik3* is capable of regulating the expression of TGFb1[39] and could also act as an antiproliferative factor.[40] We also observed *TGF-b1* induction in P15 ATF4$^{+/-}$ retina immediately after the induction of *Vegfa* at P12. Therefore, we were able to demonstrate that during retinal development the ATF4$^{+/-}$ retina experiences stronger upregulation of UPR-induced genes and transient upregulation of *Pik3r1/Akt*, *Flt1*, and *Vegfa* gene expression, thus leading to increased *Tgfb1* gene expression.

Endoplasmic reticulum stress seemed to be more robust in the C57BL/6 OIR retina. A comparison of two OIR groups demonstrated that the expression of *Bip*, *ATF6*, and *Hif1a* was lower in ATF4$^{+/-}$ OIR mice. Western blot confirmed the quantitative RT-PCT data: the levels of pAtf6-50 and pATF6-90 were reduced, suggesting a decline in the ATF6 pathways in ATF4$^{+/-}$ mice. In ATF4$^{+/-}$ OIR mice, the ATF6 signaling was not alone in being modulated: the levels of peIF2a were also diminished, indicating that PERK signaling was also downregulated.

The ATF4$^{+/-}$ OIR mice also showed a reduction in *VEGFa* and *Flt1* at P12, which later at P15 could be responsible for a reduction of *Tgfb1*. The downregulation of the VEGF protein at P13 confirms the quantitative RT-PCR data and points out the agreement between our study and work by others in which a direct link between the inhibition of VEGF and the blockage of TGFb production was proposed.[39] These data also support the finding by Liu et al.[41] demonstrating that the blockade of ATF6 in OIR neovascularization mouse models leads to an increase in intracellular VEGF degradation and a decrease in full-length intracellular VEGF, which leads to approximately a 35% reduction in angiogenesis.

Finally, the reprogramming of PERK and ATF6 signaling and the reduction of *Vegf*, *Flt1*, and *Tgfb1* in ATF4$^{+/-}$ OIR mice are associated with a reduction in neovascularization. The results from imaging analyses of new blood vessel formation were supported by counting avascular areas in the same OIR retina. The number of new capillaries in ATF4$^{+/-}$ retinas was significantly reduced, suggesting that neovascularization was retarded in these mice. Thus, our study demonstrates that a reduction in ATF4 reprograms PERK and ATF6 signaling and reduces the degree of hypoxia-driven neovascularization in OIR mice and confirms an earlier study[11] with STZ-diabetic mice. The validation of ATF4 as a potential therapeutic target holds great promise for future therapy not only for ocular neovascular disorders but also for other health conditions associated with neovascularization.

Acknowledgments

The authors thank the Riken Bioresource Center for providing the ERAI mice.

Supported by Grant R01EY020905 from the National Institutes of Health, by Grant TA-GT-0409-0508-NTERI from the Foundation Fighting Blindness, by Hope for Vision, and by Grant W81XH-10-2-0003 from the Department of Defense.

Disclosure: **X. Wang**, None; **G. Wang**, None; **M. Kunte**, None; **V. Shinde**, None; **M. Gorbatyuk**, None

References

1. Oshitari T, Fujimoto N, Hanawa K, Adachi-Usami E, Roy S. Effect of chronic hyperglycemia on intraocular pressure in patients with diabetes. *Am J Ophthalmol*. 2007;143:363–365.
2. Oshitari T, Polewski P, Chadda M, et al. Effect of combined antisense oligonucleotides against high-glucose– and diabetes-induced overexpression of extracellular matrix components and increased vascular permeability. *Diabetes*. 2006;55:86–92.
3. McAlpine CS, Bowes AJ, Werstuck GH. Diabetes, hyperglycemia and accelerated atherosclerosis: evidence supporting a role for endoplasmic reticulum (ER) stress signaling. *Cardiovasc Hematol Disord Drug Targets*. 2010;10:151–157.
4. Oshitari T, Hata N, Yamamoto S. Endoplasmic reticulum stress and diabetic retinopathy. *Vasc Health Risk Manag*. 2008;4:115–122.
5. Thuerauf DJ, Marcinko M, Gude N, et al. Activation of the unfolded protein response in infarcted mouse heart and hypoxic cultured cardiac myocytes. *Circ Res*. 2006;99:275–282.
6. Mujcic H, Rzymski T, Rouschop KM, et al. Hypoxic activation of the unfolded protein response (UPR) induces expression of the metastasis-associated gene LAMP3. *Radiother Oncol*. 2009;92:450–459.
7. Ameri K, Harris AL. Activating transcription factor 4. *Int J Biochem Cell Biol*. 2008;40:14–21.
8. Roybal CN, Hunsaker LA, Barbash O, Vander Jagt DL, Abcouwer SF. The oxidative stressor arsenite activates vascular endothelial growth factor mRNA transcription by an ATF4-dependent mechanism. *J Biol Chem*. 2005;280:20331–20339.
9. Zhong Y, Li J, Chen Y, et al. Activation of endoplasmic reticulum stress by hyperglycemia is essential for Müller cell–derived inflammatory cytokine production in diabetes. *Diabetes*. 2012;61:492–504.
10. Robinson R, Barathi VA, Chaurasia SS, Wong TY, Kern TS. Update on animal models of diabetic retinopathy: from molecular approaches to mice and higher mammals. *Dis Model Mech*. 2012;5:444–456.
11. Chen Y, Wang JJ, Li J, et al. Activating transcription factor 4 mediates hyperglycaemia-induced endothelial inflammation and retinal vascular leakage through activation of STAT3 in a mouse model of type 1 diabetes. *Diabetologia*. 2012;55:2533–2545.

12. Nakamura S, Imai S, Ogishima H, Tsuruma K, Shimazawa M, Hara H. Morphological and functional changes in the retina after chronic oxygen-induced retinopathy. *PLoS One*. 2012;7: e32167. Available at: http://www.ncbi.nlm.nih.gov/pmc/articles/PMC3279421/. Accessed August 9, 2013.
13. Li J, Wang JJ, Yu Q, Wang M, Zhang SX. Endoplasmic reticulum stress is implicated in retinal inflammation and diabetic retinopathy. *FEBS Lett*. 2009;583:1521–1527.
14. Connor KM, Krah NM, Dennison RJ, et al. Quantification of oxygen-induced retinopathy in the mouse: a model of vessel loss, vessel regrowth and pathological angiogenesis. *Nat Protoc*. 2009;4:1565–1573.
15. Nakamura S, Takizawa H, Shimazawa M, et al. Mild endoplasmic reticulum stress promotes retinal neovascularization via induction of BiP/GRP78. *PLoS One*. 2013;8:e60517. Available at: http://www.ncbi.nlm.nih.gov/pmc/articles/PMC3609792/. Accessed August 9, 2013.
16. Kunte MM, Choudhury S, Manheim JF, et al. ER stress is involved in T17M rhodopsin-induced retinal degeneration. *Invest Ophthalmol Vis Sci*. 2012;53:3792–3800.
17. Smith LE, Wesolowski E, McLellan A, et al. Oxygen-induced retinopathy in the mouse. *Invest Ophthalmol Vis Sci*. 1994;35: 101–111.
18. Choudhury S, Bhootada Y, Gorbatyuk O, Gorbatyuk M. Caspase-7 ablation modulates UPR, reprograms TRAF2-JNK apoptosis and protects T17M rhodopsin mice from severe retinal degeneration. *Cell Death Dis*. 2013;4:e528. Available at: http://www.ncbi.nlm.nih.gov/pmc/articles/PMC3613823/. Accessed August 9, 2013.
19. Rapaport DH, Wong LL, Wood ED, Yasumura D, LaVail MM. Timing and topography of cell genesis in the rat retina. *J Comp Neurol*. 2004;474:304–324.
20. Firtina Z, Duncan MK. Unfolded protein response (UPR) is activated during normal lens development. *Gene Expr Patterns*. 2011;11:135–143.
21. Zhang X, Szabo E, Michalak M, Opas M. Endoplasmic reticulum stress during the embryonic development of the central nervous system in the mouse. *Int J Dev Neurosci*. 2007;25:455–463.
22. Blackshaw S, Harpavat S, Trimarchi J, et al. Genomic analysis of mouse retinal development. *PLoS Biol*. 2004;2:E247. Available at: http://www.ncbi.nlm.nih.gov/pmc/articles/PMC439783/. Accessed August 15, 2013.
23. Vecino E, Hernandez M, Garcia M. Cell death in the developing vertebrate retina. *Int J Dev Biol*. 2004;48:965–974.
24. Yan S, Zheng C, Chen ZQ, et al. Expression of endoplasmic reticulum stress-related factors in the retinas of diabetic rats [published online ahead of print August 28, 2011]. *Exp Diabetes Res*. doi:10.1155/2012/743780.
25. Jacot JL, Sherris D. Potential therapeutic roles for inhibition of the PI3K/Akt/mTOR pathway in the pathophysiology of diabetic retinopathy [published online ahead of print October 30, 2011]. *J Ophthalmol*. doi:10.1155/2011/589813.
26. Ye X, Xu G, Chang Q, et al. ERK1/2 signaling pathways involved in VEGF release in diabetic rat retina. *Invest Ophthalmol Vis Sci*. 2010;51:5226–5233.
27. Mohammad G, Mairaj Siddiquei M, Imtiaz Nawaz M, Abu El-Asrar AM. The ERK1/2 inhibitor U0126 attenuates diabetes-induced upregulation of MMP-9 and biomarkers of inflammation in the retina [published online ahead of print April 10, 2013]. *J Diabetes Res*. doi:10.1155/2013/658548.
28. Kador PF, Zhang P, Makita J, et al. Novel diabetic mouse models as tools for investigating diabetic retinopathy. *PLoS One*. 2012; 7:e49422. Available at: http://www.ncbi.nlm.nih.gov/pmc/articles/PMC3520987/. Accessed August 9, 2013.
29. Lange PS, Chavez JC, Pinto JT, et al. ATF4 is an oxidative stress–inducible, prodeath transcription factor in neurons in vitro and in vivo. *J Exp Med*. 2008;205:1227–1242.
30. Chen Y, Wang JJ, Li J, et al. Activating transcription factor 4 mediates hyperglycaemia-induced endothelial inflammation and retinal vascular leakage through activation of STAT3 in a mouse model of type 1 diabetes. *Diabetologia*. 2012;55:2533–2545.
31. O'Driscoll C, Donovan M, Cotter TG. Analysis of apoptotic and survival mediators in the early post-natal and mature retina. *Exp Eye Res*. 2006;83:1482–1492.
32. Young RW. Cell death during differentiation of the retina in the mouse. *J Comp Neurol*. 1984;229:362–373.
33. Jung YJ, Isaacs JS, Lee S, Trepel J, Neckers L. IL-1β mediated up-regulation of HIF-1α via an NFκB/COX-2 pathway identifies HIF-1 as a critical link between inflammation and oncogenesis. *FASEB J*. 2003;17:2115–2117.
34. Forsythe JA, Jiang BH, Iyer NV, et al. Activation of vascular endothelial growth factor gene transcription by hypoxia-inducible factor 1. *Mol Cell Biol*. 1996;16:4604–4613.
35. Arsham AM, Plas DR, Thompson CB, Simon MC. Akt and hypoxia-inducible factor-1 independently enhance tumor growth and angiogenesis. *Cancer Res*. 2004;64:3500–3507.
36. Zheng J, Wen Y, Song Y, et al. Activation of multiple signaling pathways is critical for fibroblast growth factor 2– and vascular endothelial growth factor–stimulated ovine fetoplacental endothelial cell proliferation. *Biol Reprod*. 2008;78:143–150.
37. Abid MR, Guo S, Minami T, et al. Vascular endothelial growth factor activates PI3K/Akt/forkhead signaling in endothelial cells. *Arterioscler Thromb Vasc Biol*. 2004;24:294–300.
38. Fujio Y, Walsh K. Akt mediates cytoprotection of endothelial cells by vascular endothelial growth factor in an anchorage-dependent manner. *J Biol Chem*. 1999;274:16349–16354.
39. Lee KS, Park SJ, Kim SR, et al. Inhibition of VEGF blocks TGF-β_1 production through a PI3K/Akt signalling pathway. *Eur Respir J*. 2008;31:523–531.
40. Hill JJ, Tremblay TL, Cantin C, O'Connor-McCourt M, Kelly JF, Lenferink AE. Glycoproteomic analysis of two mouse mammary cell lines during transforming growth factor (TGF)-β induced epithelial to mesenchymal transition. *Proteome Sci*. 2009;7:2. Available at: http://www.ncbi.nlm.nih.gov/pmc/articles/PMC2651118/. Accessed August 15, 2013.
41. Liu L, Qi X, Chen Z, et al. Targeting the IRE1α/XBP1 and ATF6 arms of the unfolded protein response enhances VEGF blockade to prevent retinal and choroidal neovascularization. *Am J Pathol*. 2013;182:1412–1424.

Investigative Ophthalmology & Visual Science